Electrochemistry

Switching of Directions of Bioelectrocatalytic Currents and Photocurrents at Electrode Surfaces by Using Hydrophobic Magnetic Nanoparticles**

*Eugenii Katz and Itamar Willner**

Magnetic particles—microspheres, nanospheres, and ferrofluids—are widely studied and applied in various fields of biology and medicine, such as magnetic targeting (drugs, genes, radiopharmaceuticals), magnetic resonance imaging, diagnostics, immunoassays, RNA and DNA purification, gene cloning, and cell separation and purification.[1] Extensive research efforts were recently directed towards the application of functionalized magnetic particles for controlling electrochemical transformations at electrode interfaces or chemical reactivity at solid supports.[2] The magnetic attraction or retraction of magnetic particles that are functionalized with redox units to and from electrode surfaces was used to switch "on" and "off" redox processes and subsequently activate/deactivate bioelectrocatalytic transformations.[3] Similarly, catalytic magnetic particles such as nickel nanoparticles were used to switch on and off electrocatalytic processes at electrode supports by using an external magnet.[4] The rotation of magnetic particles on electrode supports was reported to enhance electrocatalytic and bioelectrocatalytic processes by the hydrodynamic transport of the reacting substrates to the electrode.[5] Enhanced electrochemically generated chemiluminescence was reported in the presence of rotating magnetic particles,[6] and the system was employed for the amplified detection of DNA,[6,7] antigen–antibody complexes,[6] and cancer cells.[8] Recently, magnetic nanoparticles with a hydrophobic capping layer were employed to reversibly separate surface-confined and diffusional redox processes at electrodes.[9,10] By dissolving the hydrophobic magnetic nanoparticles in an organic phase, the magnetic nanoparticles were transported to the electrode surface with a colayer of hydrophobic solvent. This layer enabled a change of electrochemical processes of the electrode-confined species from aqueous type to organic-phase type, and the co-transport of hydrophobic substrates to the electrode surfaces allowed switchable electrocatalysis.[10]

Herein, we demonstrate the use of hydrophobic magnetic nanoparticles in a water/toluene biphasic system to switch reversibly at a fixed potential the bioelectrocatalytically and photoelectrochemically generated currents from cathodic to anodic directions.

Magnetite nanoparticles (diameter ca. 5 nm, saturation magnetization ca. 36.4 emu g^{-1}) functionalized with a monolayer of undecanoic acid[9] were dissolved in toluene (1 mg mL^{-1}), and the solution was added to the electrochemical cell to yield a system in which the upper organic layer was immiscible with the aqueous electrolyte solution. In the first system (Scheme 1), a gold surface placed at the bottom of the electrochemical cell was modified with the hemo-undecapeptide microperoxidase-11 (MP-11; **1**) by covalent linkage of MP-11 to a monolayer of cystamine.[11] Glucose oxidase (GOx, 1 mg mL^{-1}), glucose (50 mM), and H_2O_2 (50 mM) were added to the aqueous electrolyte solution. The upper toluene phase contained the hydrophobic magnetic nanoparticles and decamethylferrocene (**2**; 2 mM). When the external magnet was positioned above the electochemical cell, the magnetic nanoparticles were confined to the organic phase and the system adopted the configuration shown in

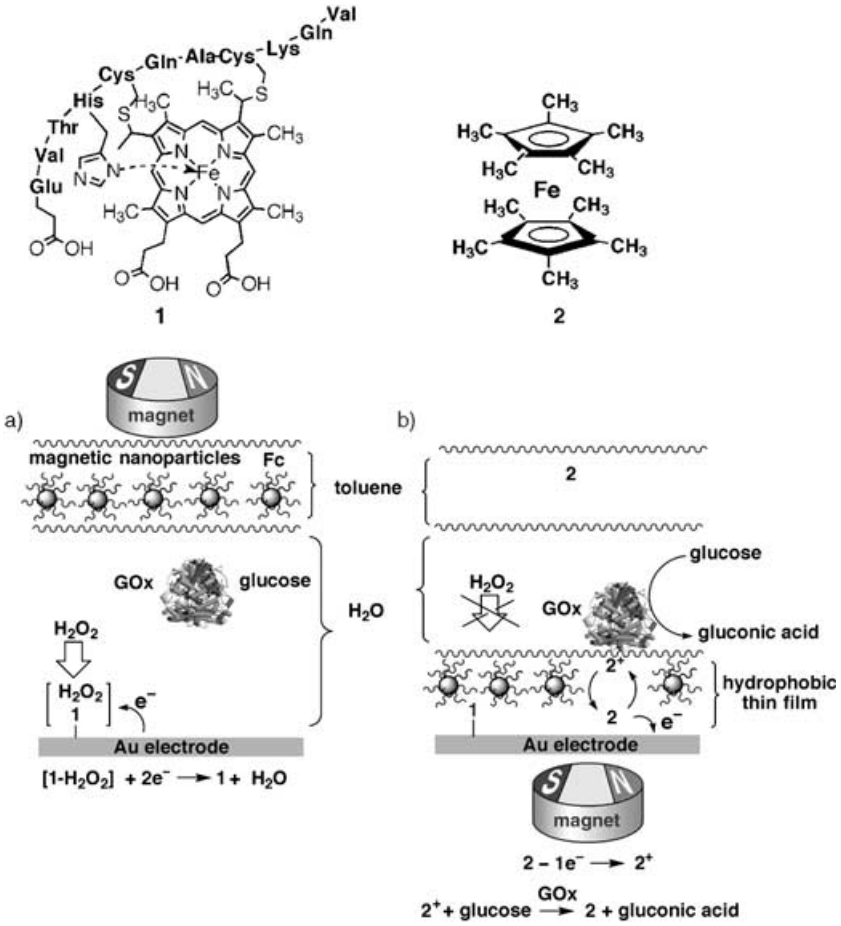

Scheme 1. Magnetoswitchable anodic/cathodic currents generated at the electrode functionalized with microperoxidase-11 (**1**) by using hydrophobic magnetic nanoparticles to gate the bioelectrocatalytic processes.

[*] Dr. E. Katz, Prof. I. Willner
Institute of Chemistry
The Hebrew University of Jerusalem
Jerusalem 91904 (Israel)
Fax: (+972) 2-652-7715
E-mail: willnea@vms.huji.ac.il

[**] This research is supported by the Israel–China Binational Program, The Israel Ministry of Science.

 DOI: 10.1002/ange.200501126

Scheme 1a. The cyclic voltammogram of the system is depicted in Figure 1a, curve 2. The electrocatalytic cathodic wave that starts at approximately 0.35 V is attributed to the electrocatalyzed reduction of H_2O_2 by **1**, as previously shown.[11a] In the absence of H_2O_2 in the aqueous phase, the cyclic voltammogram recorded at positive potentials shows a background current (Figure 1a, curve 1) while the quasi-reversible redox wave of the surface-confined MP-11 (**1**) is observed at negative potentials ($E^\circ = -0.4$ V; $\approx 1.4 \times 10^{-10}$ mole cm^{-2} surface coverage of **1**; Figure 1b). The shift in the reduction potential of H_2O_2 relative to the quasi-reversible wave of **1** observed in the absence of H_2O_2 was attributed to the formation of a complex between H_2O_2 and the heme center of MP-11 (**1**) that stimulated the reduction of H_2O_2 at the positive potentials.[11a]

Positioning of an external magnet below the electrode attracted the hydrophobic magnetic nanoparticles to the electrode. The magnetic attraction of the hydrophobic magnetic nanoparticles, which were associated with a layer of toluene that also includes **2**, to the electrode surface resulted in the cyclic voltammogram shown in Figure 1c, curve 3. In the absence of glucose in the aqueous phase, the quasi-reversible cyclic voltammogram of **2** associated with the hydrophobic magnetic nanoparticles was detected (Figure 1c, curve 2; the low voltammetric response is due to the slow scan rate). The electrocatalytic anodic current shown in Figure 1c, curve 3, is attributed to the bioelectrocatalytic oxidation of glucose by GOx mediated by **2**; that is, the oxidation of **2** in the toluene film yields the respective ferrocenyl cation that mediates the oxidation of glucose by GOx (Scheme 1b). Note, however, that upon attraction of the magnetic nanoparticles to the electrode surface, the electrocatalyzed reduction of H_2O_2 by **1** is totally blocked as a result of the formation of the hydrophobic thin film on the electrode which impedes contact between H_2O_2 dissolved in the aqueous phase and the **1**-functionalized electrode. Indeed, in the absence of **2** in the toluene phase and upon magnetic attraction of the nanoparticles from the organic phase to the electrode surface, the system shows complete blocking of the currents as a result of the isolation of the electrode surface by the hydrophobic thin film (Figure 1c, curve 1).

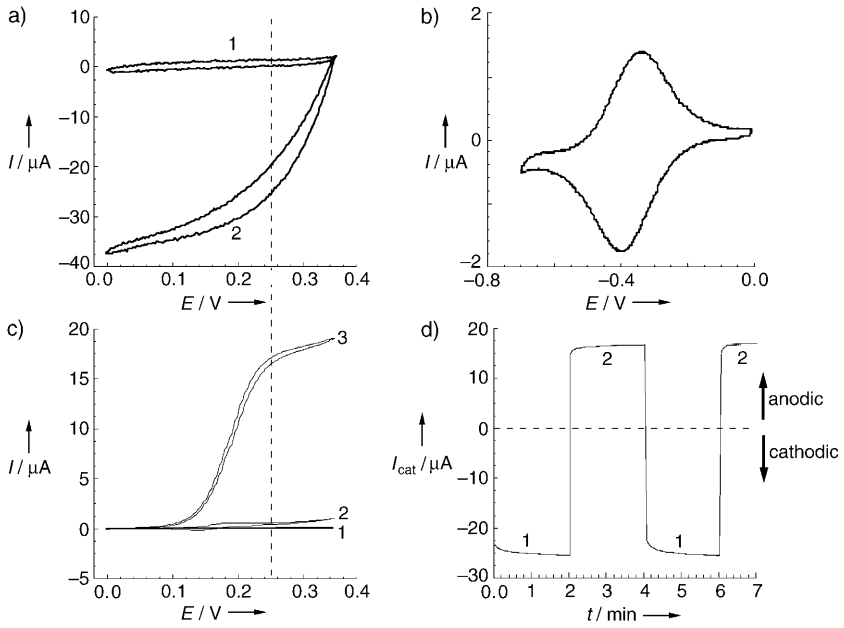

Figure 1. a) Cyclic voltammograms (potential scan rate: 5 mV s^{-1}) recorded in the presence of the **1**-functionalized electrode when the magnetic nanoparticles are retracted from the surface: 1) in the absence of H_2O_2 and 2) in the presence of H_2O_2 (50 mM). b) Cyclic voltammogram of the **1**-functionalized electrode recorded in the absence of H_2O_2 at a potential scan rate of 100 mV s^{-1}. c) Cyclic voltammograms (potential scan rate: 5 mV s^{-1}) recorded in the presence of the **1**-functionalized electrode when the magnetic nanoparticles are attracted to the surface: 1) in the absence of decamethylferrocene (**2**) in the toluene phase, 2) in the presence of **2** (2 mM) in the toluene phase and the absence of glucose in the aqueous phase, and 3) in the presence of **2** (2 mM) in the toluene phase and of glucose (50 mM) in the aqueous phase. d) Switchable bioelectrocatalytic currents generated in the system upon application of a fixed potential at 0.25 V, in the presence of H_2O_2 (50 mM) and glucose (50 mM) in the aqueous phase and **2** (2 mM) in the toluene phase, when the magnetic nanoparticles are retracted from the surface (1) or attracted to the surface (2). The data were recorded in a solution of phosphate buffer (0.1 M, pH 7.0) containing GOx (1 mg mL^{-1}).

The selective activation of the bioelectrocatalyzed reduction of H_2O_2 (by **1**) or the bioelectrocatalyzed oxidation of glucose (by **2** and GOx) enables the selection of a fixed potential value (e.g. 0.25 V vs. SCE) at which the direction of the current at the electrode surface can be reversibly switched by the hydrophobic magnetic nanoparticles (Figure 1d). When the nanoparticles are retracted from the electrode surface (Figure 1d, domains 1), the bioelectrocatalyzed reduction of H_2O_2 by **1** proceeds and a cathodic current of approximately -25 μA is observed at the applied potential of 0.25 V. Attraction of the magnetic nanoparticles to the electrode surface blocks the electrocatalytic reduction of H_2O_2, but the ferrocene-mediated bioelectrocatalyzed oxidation of glucose by GOx proceeds (Figure 1d, domains 2). A bioelectrocatalytic anodic current of about 15 μA is observed in the system at the applied potential of 0.25 V. By the cyclic retraction and attraction of the magnetic nanoparticles from or to the electrode surface, the current is switched between cathodic and anodic values, respectively.

By using a similar concept, the photoelectrochemical currents generated upon the illumination of a layer of CdS nanoparticles associated with an electrode could be switched between cathodic and anodic photocurrents by means of the hydrophobic magnetic particles (Scheme 2). A monolayer of CdS nanoparticles (diameter 5 nm) functionalized with a layer of 3-mercaptopropionic acid/3-mercaptoethanesulfonic acid was covalently linked to a cystamine-functionalized gold electrode.[12] Parallel microgravimetric quartz-crystal microbalance measurements indicated a surface coverage of approximately 3×10^{12} particles cm^{-2}. The system comprised the electrode functionalized with CdS nanoparticles and a biphasic system composed of an aqueous solution of triethanolamine (TEOA; 20 mM) as electron donor in phosphate

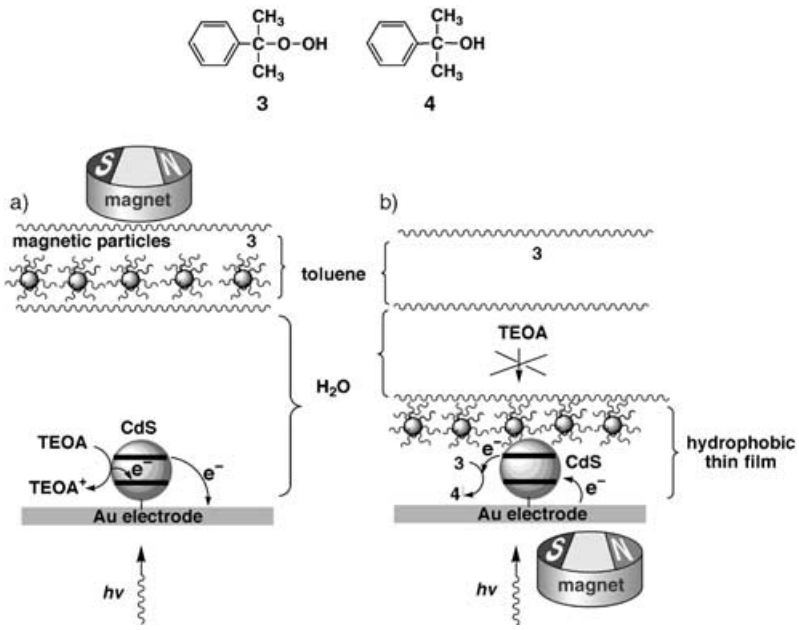

Scheme 2. Magnetoswitchable anodic/cathodic photocurrents generated at the electrode functionalized with CdS nanoparticles by using hydrophobic magnetic nanoparticles to gate the photoelectrochemical processes.

buffer (0.1 M, pH 7.0) and a solution in toluene of cumene hydroperoxide (**3**; 2 mM) and the hydrophobic magnetic nanoparticles (Scheme 2a).

Irradiation of the CdS nanoparticles through a semitransparent gold-coated glass electrode, while confining the magnetic nanoparticles to the toluene phase, resulted in an anodic photocurrent (Figure 2a, curve 1). This photocurrent is generated only if TEOA is dissolved in the aqueous medium. The photocurrent action spectrum follows the absorbance spectrum of the CdS nanoparticles, which implies that it originates from the photoexcitation of the nanoparticles; that is, upon irradiation of the CdS nanoparticles an electron–hole pair is generated. The oxidation of TEOA by the holes and the transport of the conduction-band electrons to the electrode result in the formation of the anodic photocurrent (Scheme 2a).

The magnetic attraction of the hydrophobic magnetic nanoparticles from the toluene phase containing **3** to the electrode resulted in a cathodic photocurrent (Scheme 2b and Figure 2a, curve 3). In the absence of **3** in the toluene phase, no photocurrent was generated (Figure 2a, curve 2). Thus, the cathodic photocurrent originates from the transfer of the photoexcited conduction-band electrons in CdS nanoparticles to cumene hydroperoxide (**3**) to yield the respective reduction product cumene alcohol **4** and the concomitant transfer of electrons from the electrode to the semiconductor valence-band holes (Scheme 2b). Thus, the magnetic attraction of the hydrophobic magnetic nanoparticles to the surface functionalized with CdS nanoparticles results in the blocking of the electrode surface towards the aqueous solution of TEOA, while allowing the contact of the electrode surface with the electron acceptor **3** associated with the generated hydrophobic thin film. By the cyclic attraction and retraction of the magnetic nanoparticles to and from the electrode surface, the photocurrents generated by the semiconductor nanoparticles are switched between cathodic and anodic directions, respectively (Figure 2b). The quantum yields for the generation of photocurrents (taking into account the light flux, its reduction by the semitransparent electrode, and the absorbance of the CdS monolayer) were estimated to be approximately 5% and 3% for the anodic and cathodic photocurrents, respectively.

Note that in a previous study,[13] the direction of photocurrents at an electrode was switched between cathodic and anodic values by tethering two different chromophores (an electron acceptor or electron donor) to helical peptides associated with the electrode, and the photocurrents in this system were generated by irradiation of the system at two different wavelengths. In the present study, the switchable photocurrents originate from irradiation of the system in the same spectral region and through the control of the composition of the system at the electrode surface.

In conclusion, we have demonstrated switchable systems that can be gated between anodic and cathodic currents or photocurrents at a defined potential region or upon irradiation. To the best of our knowledge, these systems represent the first examples of inherent switchable amperometric responses that originate from the tailored local composition at the electrode interface. We believe that the results present a new concept for electron transfer at electrode surfaces and for the future design of bioelectronic and optobioelectronic systems.

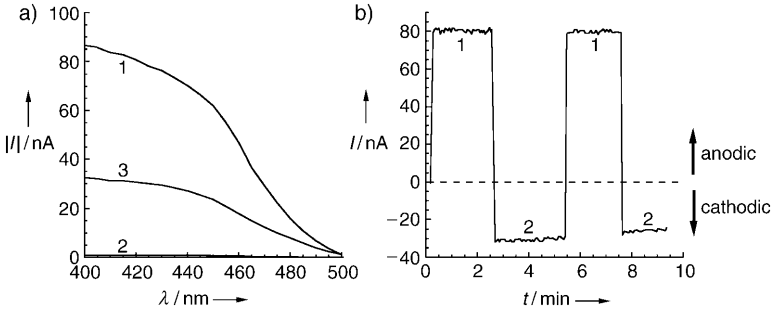

Figure 2. a) Photocurrent action spectra recorded on the electrode functionalized with CdS nanoparticles: 1) Anodic photocurrents generated when the magnetic nanoparticles are retracted from the surface; 2) cathodic photocurrents generated when the magnetic nanoparticles are attracted to the surface from the toluene phase containing cumene hydroperoxide (**3**; 2 mM); 3) no photocurrent is observed when the magnetic nanoparticles are attracted to the surface in the absence of associated **3**. b) Switchable photocurrents generated in the system upon 1) retraction from the electrode and 2) attraction to the electrode of the magnetic nanoparticles associated with **3**. The data were recorded in solutions of phosphate buffer (0.1 M, pH 7.0) containing TEOA (20 mM) and upon application of a potential of 0 V (vs. SCE).

Experimental Section

Microperoxidase-11 (**1**), glucose oxidase (GOx, EC 1.1.3.4; type X-S from *Aspergillus niger*), β-D-glucose, decamethylferrocene (**2**), cumene hydroperoxide (**3**), cystamine (2,2′-diaminodiethyldisulfide), undecanoic acid, triethanolamine (TEOA), 4-(2-hydroxyethyl)piperazine-1-ethanesulfonic acid sodium salt (HEPES), 1-ethyl-3-(3-dimethylaminopropyl)-carbodiimide (EDC), and all other chemicals were purchased from Sigma or Aldrich and used without further purification. CdS nanoparticles coated with a shell composed of 3-mercaptopropionic acid and 3-mercaptoethanesulfonic acid were prepared according to a published procedure.[12] Magnetic nanoparticles of Fe_3O_4 coated with a shell of undecanoic acid were prepared according to a published procedure except that only a single capping layer was generated on the surface of the nanoparticles.[14] Ultrapure water from NANOpure Diamond (Barnstead) was used throughout all the experiments.

A gold-coated (50-nm thick layer) glass plate (Analytical μ-Systems, Germany) was used as a working electrode. Cystamine was self-assembled on the electrode, and the resulting amine-functionalized gold electrode was treated with microperoxidase-11 (**1**; 10 mM) in HEPES buffer (0.1M, pH 7.2) in the presence of EDC (1 mM) for 2 h to yield the **1**-functionalized gold electrode.[11] Alternatively, the amine-functionalized gold electrode was treated with carboxylated CdS nanoparticles (1 mg mL^{-1}) in HEPES buffer (0.1M, pH 7.2) in the presence of EDC (1 mM) for 2 h to yield the nanoparticle-functionalized electrode.[12]

Cyclic voltammetry measurements were performed using an electrochemical analyzer (model 6310, EG&G) connected to a personal computer with EG&G 270/250 software). The photoelectrochemical measurements were performed using a homemade system that allows recording of action spectra of photocurrents.[12] The measurements were carried out at ambient temperature (25 ± 2 °C) in a conventional electrochemical cell consisting of a modified Au working electrode (0.3 cm^2 area exposed to the solution) assembled at the bottom of the electrochemical cell, a glassy carbon auxiliary electrode, and a saturated calomel electrode (SCE) connected to the working volume with a Luggin capillary. All potentials are reported with respect to this SCE reference electrode. Phosphate buffer (0.1M, pH 7.0) was used as an aqueous background electrolyte. The magnetic nanoparticles functionalized with undecanoic acid were added to the cell as a solution in toluene (0.5 mL, 1 mg mL^{-1}) to yield an immiscible system of an organic layer (upper) and the aqueous electrolyte solution (lower). Cumene hydroperoxide (**3**; 2×10^{-3} M) or decamethylferrocene (**2**; 2×10^{-3} M) was added to the toluene phase. The functionalized magnetic nanoparticles were attracted to the surface of the Au electrode from the upper organic layer by positioning a 12-mm-diameter magnet (NdFeB/Zn-coated magnet with a remnant magnetization of 10.8 kG) below the bottom electrode. The magnetic nanoparticles were removed from the electrode surface and retransported to the organic phase by positioning the external magnet above the electrochemical cell. A flow of argon through the solution was used to remove oxygen from the electrochemical cell. The cell was placed in a grounded Faraday cage.

Received: March 30, 2005
Published online: July 1, 2005

Keywords: biocatalysis · biphasic systems · magnetic properties · nanostructures · photocurrents

[1] a) *Scientific and Clinical Applications of Magnetic Carriers* (Eds.: U. Häfeli, W. Schütt, J. Teller, M. Zborowski), Plenum, New York, **1997**; b) *Advances in Biomagnetic Separation* (Eds.: M. Uhlén, E. Hornes, O. Olsvik), Eaton, Natick, **1994**; c) Y. H. Zhu, X. L. Yang, P. L. Li, H. Ying, *Prog. Chem.* **2003**, *15*, 512–517; d) A. M. Koch, F. Reynolds, M. F. Kircher, H. P. Merkle, R. Weissleder, L. Josephson, *Bioconjugate Chem.* **2003**, *14*, 1115–1121; e) A. K. Gupta, A. S. G. Curtis, *Biomaterials* **2004**, *25*, 3029–3040; f) D. Wang, J. He, N. Rosenzweig, Z. Rosenzweig, *Nano Lett.* **2004**, *4*, 409–413; g) A. K. Gupta, C. Berry, M. Gupta, A. Curtis, *IEEE Trans. Nanobiosci.* **2003**, *2*, 255–261.

[2] I. Willner, E. Katz, *Angew. Chem.* **2003**, *115*, 4724–4737; *Angew. Chem. Int. Ed.* **2003**, *42*, 4576–4588.

[3] a) R. Hirsch, E. Katz, I. Willner, *J. Am. Chem. Soc.* **2000**, *122*, 12053–1254; b) E. Katz, L. Sheeney-Haj-Ichia, A. F. Bückmann, I. Willner, *Angew. Chem.* **2002**, *114*, 1399–1402; *Angew. Chem. Int. Ed.* **2002**, *41*, 1343–1346; c) E. Katz, L. Sheeney-Haj-Ichia, I. Willner, *Chem. Eur. J.* **2002**, *8*, 4138–4148; d) J. Wang, A. N. Kawde, *Electrochem. Commun.* **2002**, *4*, 349–352.

[4] J. Wang, M. Musamesh, R. Laocharoensuk, *Electrochem. Commun.* **2005**, *7*, 652–656.

[5] E. Katz, I. Willner, *J. Am. Chem. Soc.* **2002**, *124*, 10290–10291.

[6] Y. Weizmann, F. Patolsky, E. Katz, I. Willner, *J. Am. Chem. Soc.* **2003**, *125*, 3452–3454.

[7] F. Patolsky, Y. Weizmann, E. Katz, I. Willner, *Angew. Chem.* **2003**, *115*, 2474–2478; *Angew. Chem. Int. Ed.* **2003**, *42*, 2372–2376.

[8] F. Patolsky, Y. Weizmann, E. Katz, I. Willner, *ChemBioChem* **2004**, *5*, 943–948.

[9] E. Katz, L. Sheeney-Haj-Ichia, B. Basnar, I. Felner, I. Willner, *Langmuir* **2004**, *20*, 9714–9719.

[10] E. Katz, R. Baron, I. Willner, *J. Am. Chem. Soc.* **2005**, *127*, 4060–4070.

[11] a) T. Lötzbeyer, W. Schuhmann, E. Katz, H.-L. Schmidt, *J. Electroanal. Chem.* **1994**, *377*, 291–0294; b) A. N. J. Moore, E. Katz, I. Willner, *J. Electroanal. Chem.* **1996**, *417*, 189–192.

[12] L. Sheeney-Haj-Ichia, S. Pogorelova, Y. Gofer, I. Willner, *Adv. Funct. Mater.* **2004**, *14*, 416–424.

[13] S. Yasutomi, T. Morita, Y. Imanishi, S. Kimura, *Science* **2004**, *304*, 1944–1947.

[14] L. Shen, P. E. Laibinis, T. A. Hatton, *Langmuir* **1999**, *15*, 447–453.

